

## Three-Dimensional Reconstructions of Tadpole Chondrocrania from Histological Sections

Gary Radice\*, Mary Kate Boggiano<sup>+</sup>, Mark DeSantis<sup>+</sup>,  
Peter Larson\*, Joseph Oppong<sup>+</sup>, Matthew Smetanick\*  
Todd Stevens<sup>+</sup>, James Tripp<sup>+</sup>, Rebecca Weber\*,  
Michael Kerckhove<sup>+</sup>, and Rafael de Sá\*

\*Department of Biology and <sup>+</sup>Department of Math and Computer  
Sciences, University of Richmond, Richmond, VA 23173

### ABSTRACT

Reconstructing three dimensional structures (3DR) from histological sections has always been difficult but is becoming more accessible with the assistance of digital imaging. We sought to assemble a low cost system using readily available hardware and software to generate 3DR for a study of tadpole chondrocrania. We found that a combination of RGB camera, stereomicroscope, and Apple Macintosh PowerPC computers running NIH Image, Object Image, Rotater, and SURFdriver software provided acceptable reconstructions. These are limited in quality primarily by the distortions arising from histological protocols rather than hardware or software.

### INTRODUCTION

It has always been difficult to visualize and analyze three dimensional (3D) histological features, when starting with two dimensional (2D) sections. Reconstructing the third dimension from slices presents problems in section registration as well as presenting the data in a way that can be readily interpreted. Nevertheless, there are good reasons for wanting to visualize the third dimension. In our case we wanted to compare the shapes of tadpole chondrocrania to find characters that may be useful in phylogenetic studies. For this project we sought to develop a system for generating three dimensional reconstructions (3DR) using relatively simple, low cost, and widely available hardware and software. Here, we summarize our effort and discuss the advantages and pitfalls of digital histological reconstructions.

### METHODS

#### Specimens

Tadpoles from various species were used, including *Hyla picta*, *Leptodactylus gracilis*, *Phyllomedusa hypochondrialis*, *Ptychohyla salvadorensis*, *Smilisca phaeota*, *Tripion petasatus*, and *Xenopus laevis*. Swimming tadpoles at various stages were killed in 3 aminobenzoic acid ethyl ester (MS 222) and subsequently fixed and stored in 4% formaldehyde, 0.01 M sodium phosphate at pH7.2-7.4. Most specimens were fixed after removing their body cavity organs, to speed fixative penetration.

#### Histology

For embedding, specimens were first washed in water, dehydrated through increasing concentrations of ethanol, cleared with Hemo-De® (Fisher Scientific) and embedded in ParaPlast Plus® (Oxford Laboratories). For sectioning, specimen blocks were

oriented to place the head dorsal side up and sectioned transverse to the body axis, beginning at the anterior tip of the head. Serial sections were cut at a fixed thickness of 10  $\mu\text{m}$ . Mean section thickness was verified by dividing the measured axial length of a chondrocranium by the number of sections obtained from that length. By this method mean section thickness was found to be within 5% of the nominal thickness. Sections were mounted on microscope slides previously coated with 3-aminopropyl triethoxy-silane (Sigma) for increased adhesion. Sections were de-waxed in Hemo-De and stained with Milligan's trichrome stain (acid fuchsin, fast green, and aniline blue, Presnell, 1997)..

To measure distortion introduced by histological technique, dimensions from 6 tadpoles were measured both before embedding and after sectioning and mounting. Measurements were made using NIH Image. Two dimensions were measured: intraocular distance between the farthest margin of each cornea, and length from anterior to base of chondrocranium.

Although we tried co-embedding external fiducial (registration) markers such as straight hairs, broom straw, or pine needles as aids to image registration, we obtained best results using the outline of the central nervous system as an internal registration marker. The CNS was easy to identify, when sectioned transversely was bilaterally symmetric, varied only gradually from section to section, and appeared in all but the anterior most sections of the head.

In some cases the fidelity of our reconstructions were assessed by comparing with whole chondrocrania in cleared and double-stained specimens prepared by the method of Dingerkus and Uhler (1977) .

### Microscopy and Image Capture

Images were captured using a stereomicroscope with phototube and 1x TV relay eyepiece connected to a Javelin single chip RGB digital camera and a Scion frame-grabber card (Scion Corporation, Frederick, Maryland) in an Apple Macintosh Quadra 700 or Centris 650 upgraded with a Daystar Digital 100 MHz PowerPC card, or with an Apple Macintosh PowerPC 7500/100 MHz.

For image capture we used the public domain image capture and analysis software NIH Image, v1.59 or 1.62b (developed at the U.S. National Institutes of Health and available on the Internet at <http://rsb.info.nih.gov/nih-image/>). For 3DR we used NIH Image and a modified version of NIH Image called Object Image v. 1.62b (<http://simon.bio.uva.nl/object-image.html>) in combination with Rotater 3.5 (available by anonymous FTP from <ftp://raru.adelaide.edu.au/rotater/rotater-3.5.ctp.hqx>). We also used SURFdriver (a demonstration version is available from <http://surfdriver.com>). The following is a brief summary of the image capture protocol. More detailed instructions can be obtained by anonymous FTP from [www.science.richmond.edu/radice/3dr](http://www.science.richmond.edu/radice/3dr).

Sections were viewed at low magnification to find the specimen profile with the largest dimensions, and that section was used to establish the microscope zoom magnification setting to ensure that all sections images would fit inside the same image window. The first section was oriented with dorsal facing toward the top of the screen and captured as a grayscale TIFF file, image magnification was calibrated against a standard scale, and the image was corrected for pixel aspect ratio, which ensured that measurements would be properly scaled in both vertical and horizontal dimensions.

The image was then corrected for brightness and contrast to optimize segmentation of cartilage. Subsequent images were then automatically calibrated by the software to the settings of the first file. This first file was then given a name and number designation, usually an abbreviation of the species name followed by 001, and saved in a unique folder. With this first image on screen, the next image in the series was captured and overlaid live with a transparent background onto the first image, so that both images could be seen at the same time. The live second image was then physically brought into registration with the first image by moving the microscope stage, the camera, or both until the outlines of the central nervous system were in optimal alignment. The aligned second image was then saved as a file named with the next number in the series. Subsequent images were collected in the same manner, using the previously aligned image as a reference. The complete set of images was then duplicated and archived onto removable storage media.

### Digital Reconstruction

Most reconstructions were done using NIH Image (or its spin-off Object Image) and SURFDriver on PowerPC Macintosh computers with 100-120 MHz 601 or 603e CPUs and 64-128 MB RAM. Recent reconstructions have been done with a G3/333 MHz PowerPC and ATI RAGE 2D/3D graphics accelerator card. All computers were equipped with 17 inch monitors.

The simplest reconstruction was that performed by NIH Image, which simply combines the individual image files into a stack and renders the completed stack of outlines as seen in a series of views from different angles. A set of automated commands (macros) is available within NIH Image which automate some of the procedures for working on a stack of images.

The first file in the series was opened and then a value of 1 was subtracted from the image, so that the darkest any pixel value could be was 254 (out of 255). Next, the mouse was used to outline the cartilage elements as seen on the monitor. Indistinct regions were checked by direct observation in the microscope and the resulting selected outline was converted to a black line with a grayscale value of 255. When the cartilage elements of that section were all outlined, the resulting image was thresholded so that pixels with grayscale value less than 254 were set to zero (white). This created an image of black cartilage outlines on a white background. This image was then converted to a binary format (2 bit image rather than 8 bit) to reduce the file size, and saved. Binary images require much less disk storage and processing memory. Each subsequent image was treated the same way to create a new set of binary image outlines, which were stored in a unique folder (subdirectory).

All of the binary images were then opened at the same time. The number of image windows that could be opened simultaneously was determined by the amount of random access memory (RAM) available on that computer. The windows were then converted to a *stack*, which links the data in each file sequentially into a single file. To save processing time and memory constraints, the stack was then cropped to reduce the window size and therefore file size. Minor adjustments in image registration were then done using a set of registration macros available for NIH Image that allow the user to define reference points or a line on each image and then rotate and scale the image to bring the reference markers into alignment. In our case, we drew a line from

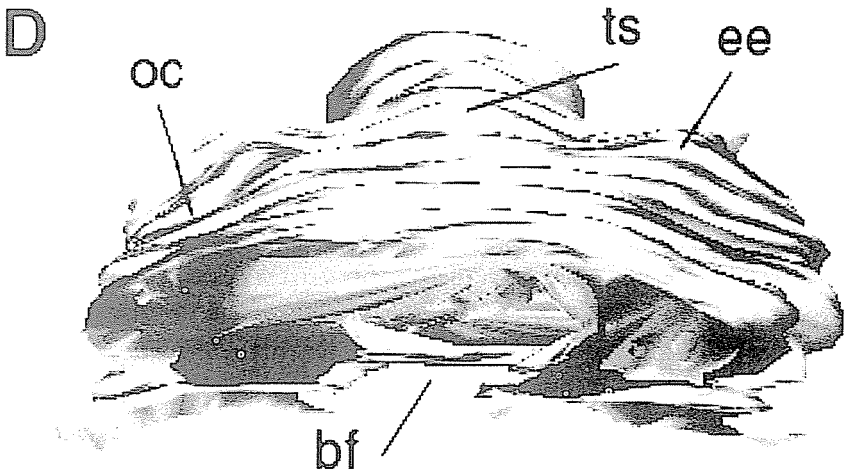
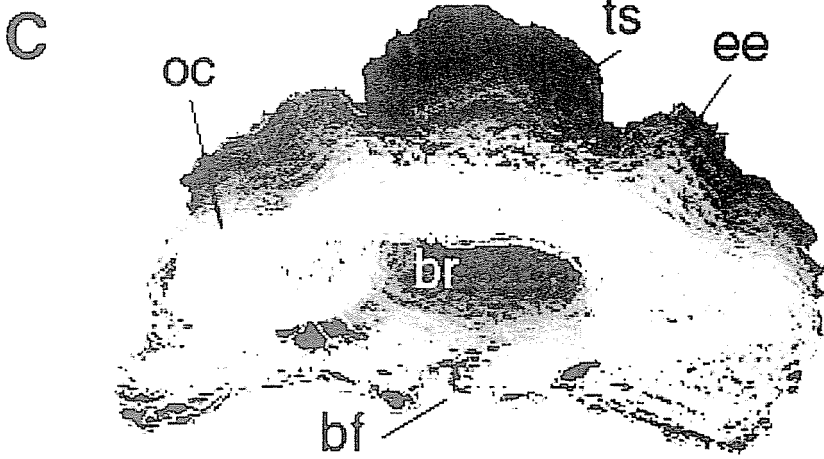
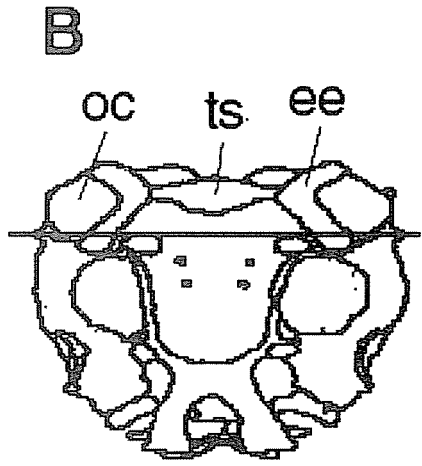
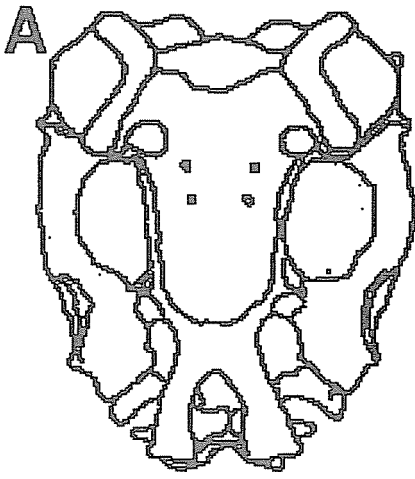


FIGURE 1. Three dimensional reconstruction of the chondrocranium of *Ptychohyala salvadorensis*. A. Camera lucida drawing of the dorsal aspect of a cleared and stained chondrocranium from a stage 41 tadpole. Anterior is toward the bottom. B. The same drawing as in A, but tilted approximately  $45^{\circ}$  to reveal the perspective seen from a dorso-anterior view similar to that of the partial reconstructions seen in C and D. Three chondrocranial landmarks are identified: oc, otic capsule; ts, tectum synoticum; ee, epiotic eminence. Only the region of the chondrocranium posterior to the crossbar was reconstructed. C. Wireframe reconstruction of the posterior chondrocranium as indicated in B. The reconstruction was created from 218 serial sections. The chondrocranial elements in each section were traced with a mouse and saved as outlines. The stack of outlines was redrawn and projected as this dorso-anterior view, shaded to enhance the illusion of depth. The reconstructed view clearly shows the ridge of the epiotic eminence (ee) and the tectum synoticum (ts). Also revealed is the cavity of the brain (br) and part of the floor of the brain case, including the basal fenestra (bf). D. A surface shell reconstruction created by SURFdriver. The same chondrocranial outlines used in C were imported into SURFdriver which creates a wireframe reconstruction and then "covers" the reconstruction with a continuous surface.

the dorsal to ventral most point of the CNS midline, which registered the sections for lateral position and rotational alignment.

To render the 3DR, the gray values were then inverted so that the images became white borders on a black background. Viewing the image this way enhanced the 3D illusion. Then, the reconstruction was created by entering the appropriate values in the *Projection* menu. Projection options and the values we used were (1) pixel spacing between slices: zero or one (2) initial angle:  $0^{\circ}$ , (3) total rotation angle:  $90^{\circ}$  for draft copies and  $360^{\circ}$  for final versions (4) rotation increment;  $5^{\circ}$ , (5) lower transparency bound: 0, (6) upper transparency bound: 254 (7) surface opacity: 0, (8) surface depth cueing: 100, (9) interior depth cueing: 50, (10) axis of rotation: X or Y, (11) projection method: brightest point. A typical projection rendering took 2-20 minutes, depending on the computer and the size of the particular stack. Once completed, the projection views were saved as NIH Image projection files or as QuickTime movies. One such projection is seen in Fig. 1C.

Object Image provided the additional feature of being able easily to separately color code various features in our outlined stacks, and then export those data to the separate program Rotater 3.5. Rotater permits mouse-controlled rotation in any axis, constructs stereo pairs, adjusts depth cues and perspectives, and several other features that aid visualization of wireframe objects.

### Reconstruction using SURFdriver

To reconstruct using SURFdriver we began with the binary outlines generated in NIH Image and converted them from TIFF to PICT format files as required by SURFdriver. Unfortunately, we also had to rename each file since SURFdriver and NIH Image use different and incompatible naming conventions to automatically recognize the correct file sequence. Then we opened SURFdriver, opened each file in sequence, and used the mouse to trace the cartilage element outlines. If we had not already outlined the cartilage elements using NIH Image, we could have captured the grayscale section images directly as PICT files and opened them directly in SURFdriver, and done the original segmentation there, saving several steps. These cartilage outlines, which SURFdriver calls contours, were then each identified with a number so that same object could be connected by the software with its corresponding outline

in previous and subsequent sections. Free ends of objects were identified and marked so that the software did not mistakenly join them to other objects.

Once objects were identified and the contours drawn on each section, SURFdriver interpolated a set of points along each contour. The contour outlines then were rendered as a wireframe view similar to that created in NIH Image. SURFdriver has the additional ability to rotate the wireframe view around any axis, not just X, Y, or Z. Furthermore, SURFdriver can apply a surface over the wireframe reconstruction. It does this by generating a mesh of triangles among the coordinates of points on contours of adjacent sections and then covering the triangular mesh with a texture map, colored and shaded to enhance the illusion of depth.

### RESULTS AND DISCUSSION

The goal of the present work was to assemble a low cost and easily used combination of hardware and software for creating accurate 3DR of tadpole chondrocrania. There were 5 problems that we addressed: (1) section distortion (2) section loss (3) image registration (4) feature segmentation (5) rendering the 3DR.

(1) We found that paraffin sectioning produced extensive distortion, mostly from section compression during sectioning. Because all of our specimens were sectioned with the dorsal/ventral axis perpendicular to the knife edge, all of our reconstructions were compressed along the dorsal/ventral axis. This compression was as much as 40%, even after floating the sections on water at 46 °C. Unfortunately, section compression is difficult to avoid. One approach is to use methacrylate plastic as an embedding medium. Plastic resists compression better than wax but it is more difficult to collect serial sections with methacrylate because it does not easily form ribbons. An entirely different solution borrows from the erosion procedure used in mineralogy, whereby a stereomicroscope and camera are mounted at the microtome to capture an image of the specimen within the block face prior to each section rather than imaging the sections after they are cut and mounted. In this way each image is captured undistorted by sectioning and moreover is precisely in register. Such a procedure was used successfully by Lozanoff (1992) to make undistorted 3DR of mouse skulls. Unfortunately, such a method can be applied only to those structures that can be visualized unstained or stained *en bloc* and viewed with epi-illumination. It is also limited to the comparatively low resolution available with a stereomicroscope. In our case we wanted higher resolution images using a compound microscope optics, which require transillumination. Although section compression therefore could not be avoided, it could be accommodated by software after image capture by proportionately scaling the images in the direction of compression, as long as the precise amount and direction of compression was known. Fortunately, both were easy to determine.

(2) Section loss was minimal. Silanized slides rarely lost sections during processing. The most common losses were those that occurred while sections were being transferred from the microtome to the water bath or to the slides, and it was easy for the operator to note which sections in a series were missing. Missing sections were accommodated in one of three ways: by incorporating a blank placeholder image in the series, by duplicating the image of the section prior to the missing one, or by adding an image that was an average of the sections before and after the missing slice. The first method preserves a record of the missing slice in the reconstruction as a gap or a step in the surface, the other methods produce a smoother surface rendering.

(3) Image registration was the most difficult problem to overcome. We chose to use the dorsal and ventral midpoints of the CNS as internal registration markers and software to assist rotating and aligning successive images with respect to these two points. This method required careful attention by the user and was not completely reliable since aligned reconstructions still showed some misplaced sections, as judged by the smoothness of the reconstructed surface (Fig 1C and D). For most tissues, and especially those without an internal symmetry, it may be necessary to co-embed an external fiducial marker. The function of such a marker is to provide a stable focal point or points in each section to which each section can be aligned. The ideal marker has a uniform cross-sectional dimension much smaller than the object of interest, is straight and does not change position from one section to the next, is oriented parallel to the direction of sectioning, and is pigmented or stainable. Having two or more such markers in each section increases their reliability. Given a stable set of fiducial marks, section rotation, lateral translocation, and even compression distortion can be compensated. We tried a number of recommended fiducial markers including strips of liver, silk thread, boar hair from a paint brush, broom straw, and needles from the white pine, *Pinus alba*. In practice, none of these markers was completely satisfactory. Liver strips were too large and difficult to produce in straight pieces. Silk threads were not straight enough. Hair, broom straw, and pine needles were straight and small enough but were difficult to infiltrate and embed, tended to crumble out of the section, and were difficult to keep parallel to each other. They might be more useful with an embedding jig to maintain colinearity of the fiducial markers. One such jig can be found in Gaunt (1978). Other methods others have used for registering sections include marking the faces of the block with carbon so that each section is outlined with carbon after mounting and staining (Ware and LoPresti 1975; Gaunt and Gaunt 1978), and shooting holes in the block with eximer lasers to create regularly spaced voids (Bron, Gremillet et al. 1990).

(4) Image segmentation, recognizing cartilage tissue in each section, proved relatively easy. Cartilage tissue structure is distinctive and among the easiest to recognize in histological section, even by novices and even in black and white. In addition, when stained with alcian blue or fast green it acquires a distinctive color that makes its identification simple.

(5) Image rendering was handled differently by the two software programs. Both programs provide useful 3D information but render it in different ways.

NIH Image creates 3DR using a projection routine that renders the object by drawing the view that would be seen if parallel rays of light passed through the object and draws an image on a screen of the pixel values intercepted along the way, according to one of three algorithms: display the brightest pixel value, the mean pixel value, or the nearest pixel value. In our images of uniformly white outlines on a black background, brightest point projections gave the most pleasing image (Fig. 1 C). Then the software rotates the stack a user-defined number of degrees about one of the three axes, and draws another view. Smaller increments and greater total rotation require longer to process initially but once completed give smoother animations. NIH Image reconstructions are simple to prepare and look best when shown in animation rather than in static images. In static images it can be difficult to differentiate those lines that are in the foreground from those in the back. Animations are limited to rotations about the X or Y axes. These limitations can be overcome partially by using the additional visualization abilities of Object Image and Rotater, such as creating stereo images that

can be viewed with 3D glasses, and false coloring of selected outlines to help distinguish connected regions.

To calculate the spacing between slices, we first determined the lateral pixel spacing based on the image magnification, which varied slightly from specimen to specimen. For example, if the lateral image scale on screen was 0.3 pixels per  $\mu\text{m}$ , then each 10  $\mu\text{m}$  thick section should occupy approximately 3.3 pixels along the Z axis. By default, however, software considers each slice to be only one pixel thick. NIH Image permits three methods to display slices that are thicker than one pixel. One method allows one to simply to insert blank pixel "spacers" to separate each slice. This approach does not increase the processing needed to render the reconstruction but it does produce a 3DR with gaps and jagged edges. A second approach is to replicate each slice an integer amount, so that each slice effectively becomes thicker. A third approach is to insert slices that average the adjacent slices. These two approaches rendered a smoother reconstruction but at the cost of increased memory requirements and slower rendering times.

Because SURFdriver can add a textured surface that covers the wireframe view, its reconstructions can appear more life-like than those of NIH Image (Fig 1D). The increased realism comes at the cost of much more tedious preliminary data entry, since the user must not only outline each contour but also identify and keep track of which contours belong to distinct objects and which are connected by branch points. This may require users to have a more sophisticated knowledge of the tissue.

Various approaches to 3DR from 2D sections have been tried since the middle of the last century (reviewed by Ware and LoPresti, 1975, and Gaunt, 1978). The first was that of Wilhelm His (1868) who created both graphic and solid model reconstructions of human embryos. In this century solid models gradually came to be replaced by overlays of transparent plates, or cinematography of serial sections that by rapidly cycling through the sections could generate a "flip-card" kinesthetic sense. In the 1960's mainframe computers and custom software were used to generate the first digital reconstructions. The advent of powerful desktop computers and widely available software in the last 10 years has greatly simplified 3DR and brought it in reach of most histology and anatomy laboratories. For some recent examples see Aferzon, (1991), Lozanoff, (1992), Hyde, (1992) Born (1994), and Moses, 1995. Yet, even with these advances, we found that creating reliable and informative 3DR from serial sections is still tedious, time consuming, and far from automatic.

Large reconstructions require large amounts of memory and rapid processors. Although we were able to create 3DR with low-end PowerPC CPUs with processors running at 100-120 MHz and 64 MB RAM, such a configuration is barely adequate to create a reconstruction of 200 slices, which can occupy many tens of megabytes. For example, a 100 MHz processor rendered a 17 megabyte NIH Image projection in about 20 minutes, but this same operation took less than three minutes on a computer with 333 MHz G3 processor and graphics accelerator. Fortunately as processor speeds continue to rise and memory prices to decline, it will become easier and cheaper to create larger 3DR faster on standard desktop machines.

#### ACKNOWLEDGEMENTS

MKB, MD, PL, JP, MS, TS, JT and RW contributed to this project as undergraduate students of the University of Richmond, and were responsible for all of the histology,



image capture, and initial image processing. GR, MK, and RdS were responsible for 3D reconstruction and interpretation of the images. The work was supported by NSF Grant BIR 9510228.

## LITERATURE CITED

- Aferzon, J., R. I. Chau and D. F. Cowan (1991). A microcomputer based system for three-dimensional reconstructions from tomographic or histologic sections. *Anal Quant Cytol Histol* 13(2): 80-8.
- Born, C. T., A. J. Mure, W. M. Iannacone and W. G. DeLong, Jr. (1994). Three-dimensional computerized tomographic demonstration of bilateral atlantoaxial rotatory dislocation in an adult: report of a case and review of the literature. *J Orthop Trauma* 8(1): 67-72.
- Bron, C., P. Grenillet, D. Launay, M. Jourlin, H. P. Gautschi, T. Bachi and J. Schupbach (1990). Three-dimensional electron microscopy of entire cells. *J Microsc* 157(Pt 1): 115-26.
- Dingerkus, G. and D. L. Uhler (1977). Enzyme clearing of alcian blue stained whole small vertebrates for demonstration of cartilage. *Stain Technol* 52: 229-232.
- Gaunt, W. A. and P. N. Gaunt (1978). *Three Dimensional Reconstruction in Biology*. Tunbridge Wells, Kent, England, Pitman Medical Publishing Co.
- His, W. (1868). *Untersuchungen fiber die erste anlage des Wirbeltierleibes*. Leipzig, F.C.W. Vogel.
- Hyde, D. M., D. J. Magliano, E. Reus, N. K. Tyler, S. Nichols and W. S. Tyler (1992). Computer-assisted morphometry: point, intersection, and profile counting and three-dimensional reconstruction. *Microsc Res Tech* 21(4): 262-70.
- Lozanoff, S. (1992). Accuracy and precision of computerized models of the anterior cranial base in young mice. *Anat Rec* 234(4): 618-24.
- Lozanoff, S., B. A. Long, D. L. Singer and J. J. Deptuch (1992). An imaging routine for assessing the efficacy of instruments used for scaling and root planing. *J Clin Periodontol* 19(8): 553-9.
- Moses, R. L., P. W. Flint, C. H. Paik, S. J. Zinreich and C. W. Cummings (1995). Three-dimensional reconstruction of the feline larynx with serial histologic sections. *Laryngoscope* 105(2): 164-8.
- Presnell, J. K. and M. P. Schreibman (1997). *Humason's Animal Tissue Techniques*. Baltimore, The Johns Hopkins University Press.
- Ware, R. W. and V. LoPresti (1975). Three-Dimensional Reconstruction from Serial Sections. *International Review of Cytology* 40: 325-440.

